ANALYSIS OF AUTONOMOUS SEAWATER pH DATA AND INSTRUMENT CALIBRATION VERIFICATION METHOD

A THESIS SUBMITTED TO
THE GLOBAL ENVIRONMENTAL SCIENCE
UNDERGRADUATE DIVISION IN PARTIAL FULFILLMENT
OF THE REQUIREMENTS FOR THE DEGREE OF

BACHELOR OF SCIENCE

IN

GLOBAL ENVIRONMENTAL SCIENCE

AUGUST 2016

By
ERIC WADNAL

Thesis Advisor

ERIC HEINEN DE CARLO

I certify that I have read this thesis and that, in my opinion, it is satisfactory in scope and quality as a thesis for the degree of Bachelor of Science in Global Environmental Science.

THESIS ADVISORS

Eric Heinen De Carlo
Department of Oceanography

For my family and friends, and those willing to study and appreciate the extraordinary value of our environment.

ACKNOWLEDGEMENTS

I would like to thank, first and foremost, Eric De Carlo for his guidance and advice for this project. I’ve gained writing skills, laboratory skills, work ethic, and knowledge from him that I will be able to use in many aspects of my future. He gave me the resources and guidance I needed for this thesis while still giving me the freedom to shape it into something that is my own work. Additionally I would like to acknowledge the assistance I have received from my fellow lab mates in the Ocean Acidification research lab, particularly Gerianne Terlouw and Ryan Tabata.

I want to address the hard work of Michael Guidry throughout my time in the Global Environmental Science (GES) Program. He has helped me stay on track for this project and for all of the classes I needed for this program. He always checked in with my progress and would never hesitate to take time out of his schedule to assist me with any issues whatsoever.

I would like to thank all of my professors I’ve had while in the GES program for giving me invaluable knowledge and skills that have given me a great appreciation for science and a thorough understanding of climate change and the environment. And finally I want to thank my friends and family for their support in this program and throughout my schooling.

ABSTRACT

Recently ocean acidification (OA) has received increased attention from scientists due to its potential adverse effects on marine ecosystems, so obtaining an accurate and precise pH measurement in the coastal ocean is critical. This project aims to obtain the most precise pH measurements possible using a pH spectrophotometer, and will use these measurements to correct time series data collected by three PMEL MAPCO$_2$ buoys around Oahu and determine the data's reliability. Two of the buoys are located on fringing reefs of the south shore and one on the barrier reef in Kaneohe Bay. Other parameters with time series data are then used to analyze influences on the coastal pH around Oahu. For each buoy location, bottle samples were collected in situ at times corresponding to when the SeaFET, a pH instrument attached to the buoy, is programmed to measure pH. Bottle data were used to calibrate the time series data collected by the SeaFET. Spectrophotometrically measured pH differed from the SeaFET measurements by a small, yet significant value.

Analysis of the data shows positive correlations between pH and dissolved oxygen at both south shore buoys, as well as a less well defined relationship with chlorophyll and turbidity. There are also clear diel cycles in pH due to photosynthesis, and seasonal changes in the times at which pH peaks each day. The pH data collected at each of the three locations can be considered reliable based on the spectrophotometric measurements, and each of the three locations isa influenced by slightly varying factors.

TABLE OF CONTENTS

1.0 INTRODUCTION

1.1 OCEAN ACIDIFICATION

Recently ocean acidification (OA) has received increased attention from scientists due to its potentially adverse effects on marine ecosystems. Ocean acidification occurs as the pH of seawater decreases, so accurately measuring pH (and its variations) in seawater is critical to understanding OA. Due to human activity, the pH in the surface ocean is now 0.1 units less than preindustrial levels, and could decrease by another 0.3 to 0.4 units by 2100 based on emission scenarios that lead to atmospheric CO_2 levels that could potentially reach 800ppm (Orr et al. 2005). This decrease translates to hydrogen ion concentrations [H+] that are currently about 21% higher than preindustrial values, and predicted 2100 pH values that are 50-60% lower than now ($pH=-\log_{10}[H^+]$, $[H^+]=10^{pH}$).

Calcifying organisms may be threatened by a decrease in carbonate ion concentrations and pH that results from increased concentrations of dissolved CO_2 in seawater, which also leads to increases in bicarbonate ions (HCO_3^-) (de Putron et al. 2011). Scientists have most commonly used carbonate ions (CO_3^{2-}) as a proxy to determine the saturation state of seawater (e.g. Orr et al. 2005). However, most calcifying organisms use CO_2 and HCO_3^- as a calcifying substrate (Roleda et al. 2012), and a stronger correlation to calcification could be obtained by using the ratio between [HCO_3^-] and [H+] referred to as the substrate-to-inhibitor ratio, or SIR (Fassbender et al 2016). The concentration of CO_2 in the atmosphere is near equilibrium with the amount of CO_2 that is dissolved in the surface ocean, and when the atmospheric concentration increases, more CO_2 is absorbed by the ocean, and vice versa. Dissolved CO_2 reacts with water and forms carbonic acid, H_2CO_3, which then dissociates into bicarbonate, HCO_3^-, and to a much lesser extent into carbonate ions, CO_3^{2-}. As a result of dissociation, more H+ ions are present to react with CO_3^{2-} already in seawater, thereby reducing the availability of CO_3^{2-} for use by organisms to form their calcium carbonate ($CaCO_3$) structures.

Increased H+ is therefore the cause of increased acidity (i.e. a decrease in pH), and as [H+] increases, the concentration of CO_3^{2-} decreases, a phenomenon known as OA (see Figure 1). This lowered SIR is a fundamental problem for calcifiers associated with OA. The following equations represent the series of reactions after CO_2 is dissolved into seawater:

$$CO_{2\,(aq)} + H_2O \leftrightarrow H_2CO_3 \leftrightarrow HCO_3^- + H^+ \leftrightarrow CO_3^{2-} + 2\,H^+ \qquad \text{Eq. 1}$$

$$H_2CO_3 + CO_3^{2-} \rightarrow 2HCO_3^- \qquad \text{Eq. 2}$$

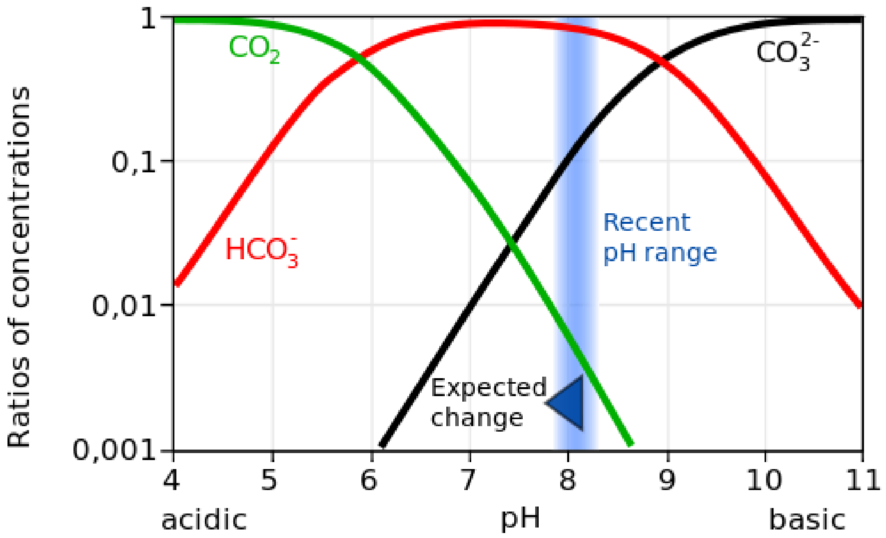

Figure 1 - Ratios of concentrations of important carbonate species in seawater

1.2 IMPACTS OF OA ON MARINE ECOSYSTEMS

The process of calcification can be strongly affected by OA, leading to enhanced susceptibility of calcifying organisms, which often are an integral part of the marine food web. Reduced calcification rates or increased dissolution rates have been measured in some types of corals, plankton, bivalves, and molluscs (Kroeker et al. 2010). Pteropods, a group of plankton that are major producers of aragonite (a form of calcium carbonate) and are negatively impacted by OA, are an example of one type of calcifying organism whose abundance could greatly affect certain marine ecosystems, because pteropods are integral to the base of the food web (Fabry et al. 2008). These authors report that in high latitude regions, shelled pteropods may reach densities from 1,000 to greater than10,000 m^{-3}. In under-saturated conditions with respect to aragonite, the concentration of calcium and carbonate ions in seawater is not at equilibrium with respect to aragonite solubility ($CaCO_3$), so aragonite cannot form and dissolves. Like other calcifying organisms, pteropods are put under stress in under-saturated conditions (see Figure 2) (Orr et al. 2005). A reduced abundance of pteropods could have serious implications to pink salmon, for example, which rely on pteropods to feed. A study by Willette et al. 2001 showed higher a mortality of juvenile pink salmon when there was not a pteropod bloom, which also keep the juveniles in near-shore habitats where they are less threatened. There are many other organisms that feed on pteropods, and the entire structure and diversity of marine ecosystems could therefore be altered by the changing carbonate chemistry occurring in the ocean.

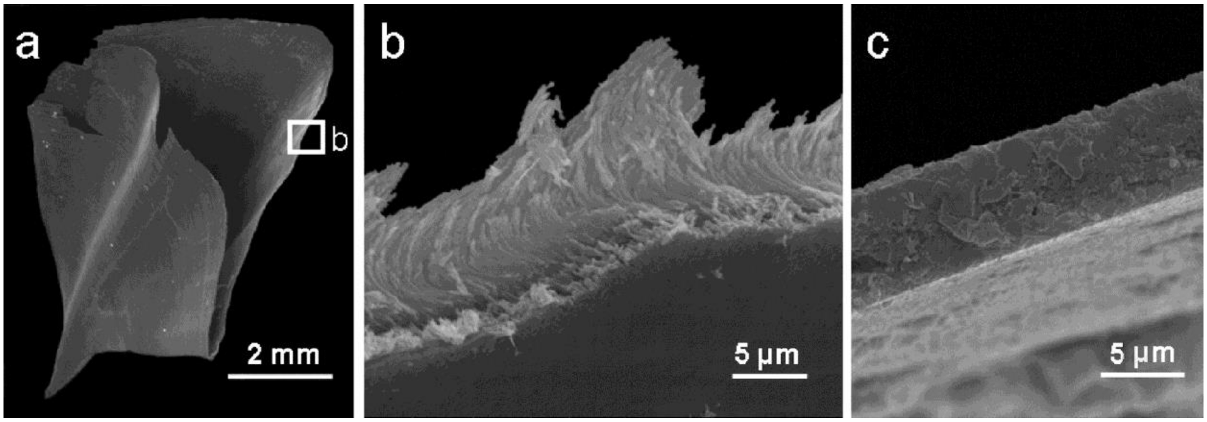

Figure 2 - SEM of Pteropod shell, (a) whole shell in water undersaturated with respect to aragonite, (b) close up of shell in under saturated and (c) over saturated conditions (Fabry et al. 2008)

In addition to calcifying plankton, lower calcification results from lower carbonate concentrations (which results from OA) in nearly all reef-building corals (Feely et al. 2004). Coral reefs serve as a critical habitat for a large variety of species in tropical regions including fish, a very important commodity in Hawaii, and if the health of coral reef declines significantly due to ocean acidification, it is likely that there will be negative environmental and economic impacts as well.

Healthy corals and coral reef ecosystems are an important source of revenue for Hawaii’s tourist industry. Annually, Hawaiian coral reefs generated around $304 million per year from recreation and tourism (Cesar et al. 2004). Near-shore coral reefs also provide shoreline protection from waves and generate coral sand (Cesar et al 2014). Additionally, small-scale fishing in Hawaii has important cultural significance, and although overfishing is another important problem that needs to be addressed, fishing still contributes economic value to Hawaii.

Ocean acidification will also impact the distribution of many species. Based on regional changes in aragonite saturation and plankton distributions, pteropods will be among the first groups of plankton to be exposed to persistently undersaturated seawater. Impacts to species distribution are expected to occur both vertically in the water column and latitudinally (Fabry et al 2008). The impact of OA on plankton species distribution could have serious consequences for marine ecosystems due to the importance of plankton as the foundation of the marine food web. Any changes in their distribution could affect the distribution of larger species that are dependent on specific food sources both temporally and spatially. Therefore it is important to understand OA through accurate measurments of pH in a multitude of locations in the world ocean.

1.3 FACTORS DRIVING COASTAL OCEAN pH

While long-term surface ocean pH changes are primarily caused by changes in atmospheric CO_2 concentrations, biological processes cause important daily fluctuations in pH. A clear 24-hour cycle is exhibited by pH due to changes in the relative rates of photosynthesis and respiration. A study by Hendriks et al. (2013) examined the variability in the pH of a coastal seagrass meadow, where the seagrass photosynthesizes and acts as a buffer to OA. The clear diel cycle in pH and dissolved oxygen that results from seagrass photosynthesis can be seen in Figure 3. The pH of the water increases during the day as CO_2 is taken up by phytoplankton, and pH decreases at night as CO_2 is replenished by respiration and diffusion from the atmosphere (Wootton et al. 2008). Ocean pH variability also exists on seasonal and yearly timescales, however these patterns are much more complex. Seasonal patterns are based on a tendency of the abundance of phytoplankton to decline in the summer, which would reduce CO_2 uptake and lower pH; as well as increased seawater temperature and lower atmospheric CO_2 in the summer, which causes transfer of CO_2 out of seawater ind increases pH (Wootton et al. 2008).

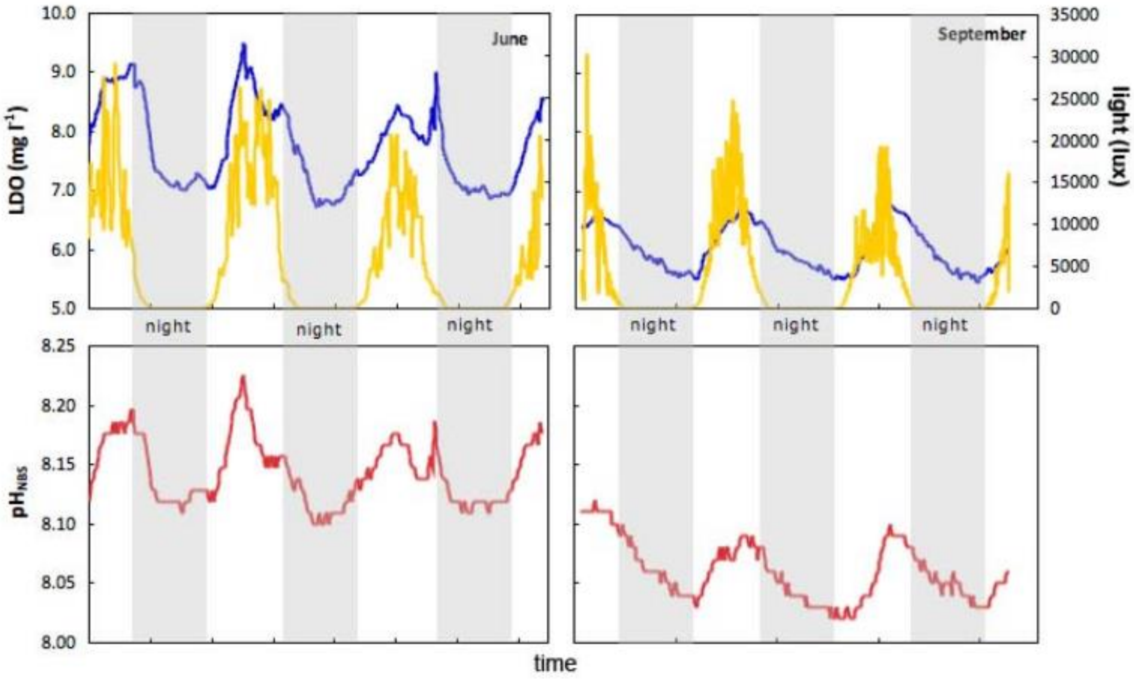

Figure 3 - Diurnal profiles of light level, oxygen, and pH in a coastal seagrass meadow. The pH follows the diel pattern with oxygen peaking when there is more light. Seasonal differences are also apparent with less oxygen, and therefore lower pH, observed in September compared to June (Hendriks et al. 2013).

Biological activity near coastlines is also largely regulated by inputs from terrestrial surface water that flows into the ocean. The rate of marine primary production is governed by light, temperature, and the availability of nutrients. When production rates increase, the pH of the water becomes more basic due to the removal of CO_2 via photosynthesis. In contrast, respiring organisms lower the pH by producing CO_2, and respiration has the greatest relative influence at night. Agriculture, golf courses, and urbanized areas, all found on the island of Oahu, contribute runoff containing nutrients, which fuel biological activity in the coastal ocean. The degree and spatial extent to which coastal ocean pH is influenced by urbanization will also depend on various factors such as population density, land use, rainfall/runoff, and water treatment and discharge.

1.4 OBJECTIVES

The primary objective of this project is to obtain a better understanding of coastal ocean dynamics by conducting an analysis of the pH time series data collected by three Pacific Marine Environmental Laboratory (PMEL) MAPCO$_2$ buoys around Oahu. Two of the buoys are located on fringing reefs of the south shore and one is on the barrier reef in Kaneohe Bay. The data were compared to climatic and other seawater parameters also collected by the PMEL buoys, including temperature, precipitation, turbidity, chlorophyll fluorescence, and dissolved oxygen concentration. Correlations between pH and any of these other parameters may indicate potential influences of the parameter on pH fluctuations.

The second objective of this project is to develop a method to calibrate the pH time series measurements collected by the SeaFET instruments. Bottle samples were collected at the three buoys at times corresponding to when the SeaFET is programmed to measure pH. The pH of seawater was measured promptly using the highly precise and accurate spectrophotometric method developed by Dickson et al. 2009. Analysis of the bottle sample and buoy measurements may be used to develop a calibration function that can then be applied to autonomously collected data to correct the pH. When corresponding dissolved inorganic carbon (DIC) and total alkalinity (TA) samples exist, the pH measurements made autonomously and made on seawater samples were compared with the pH calculated from TA and DIC using CO$_2$SYS, a program developed for calculating inorganic carbon system parameters (Pelletier 2007). Ultimately this will improve the reliability of *in situ* measurements and validate buoy data.

2.0 METHODS

2.1 BUOY LOCATIONS

Data from three buoys were used in this project. Two are located on the south shore, “leeward” side of Oahu, and one is located in Kaneohe Bay on the Northeast, or “windward” side of Oahu (see Figure 4). The two south shore sites, Ala Wai (21.28°N, 157.85°W) and Kilo Nalu (21.29°N, 157.87°W) are situated 200m offshore above fringing reefs along an open coast and are consistently exposed to physical effects of wind, open ocean waves, and tides. Although Ala Wai and Kilo Nalu are in relatively close proximity, approximately 1.6 km apart, t9he most important difference between the two is that the Ala Wai site receives freshwater river) effluent from the Ala Wai Canal. The Ala Wai Canal discharge contains a significant amount of suspended solids and nutrients, input of which has the potential to dramatically change the near-shore seawater chemistry, whereas Kilo Nalu does not receive direct riverine input (See Figure 4).

Kaneohe Bay is the largest semi-enclosed body of water on Oahu and is confined by the only true barrier reef of Oahu. The buoy in Kaneohe Bay, CRIMP2 (21.46°N, 157.80°W), was deployed at the edge of the barrier reef in about 3 m of water (See Figure 4). The purpose of this location is to measure chemical changes made to ocean water flowing into the bay over the barrier reef. An important feature that distinguishes CRIMP2 from Ala Wai and Kilo Nalu, among others, is that its location is far offshore and is therefore not directly affected by freshwater runoff.

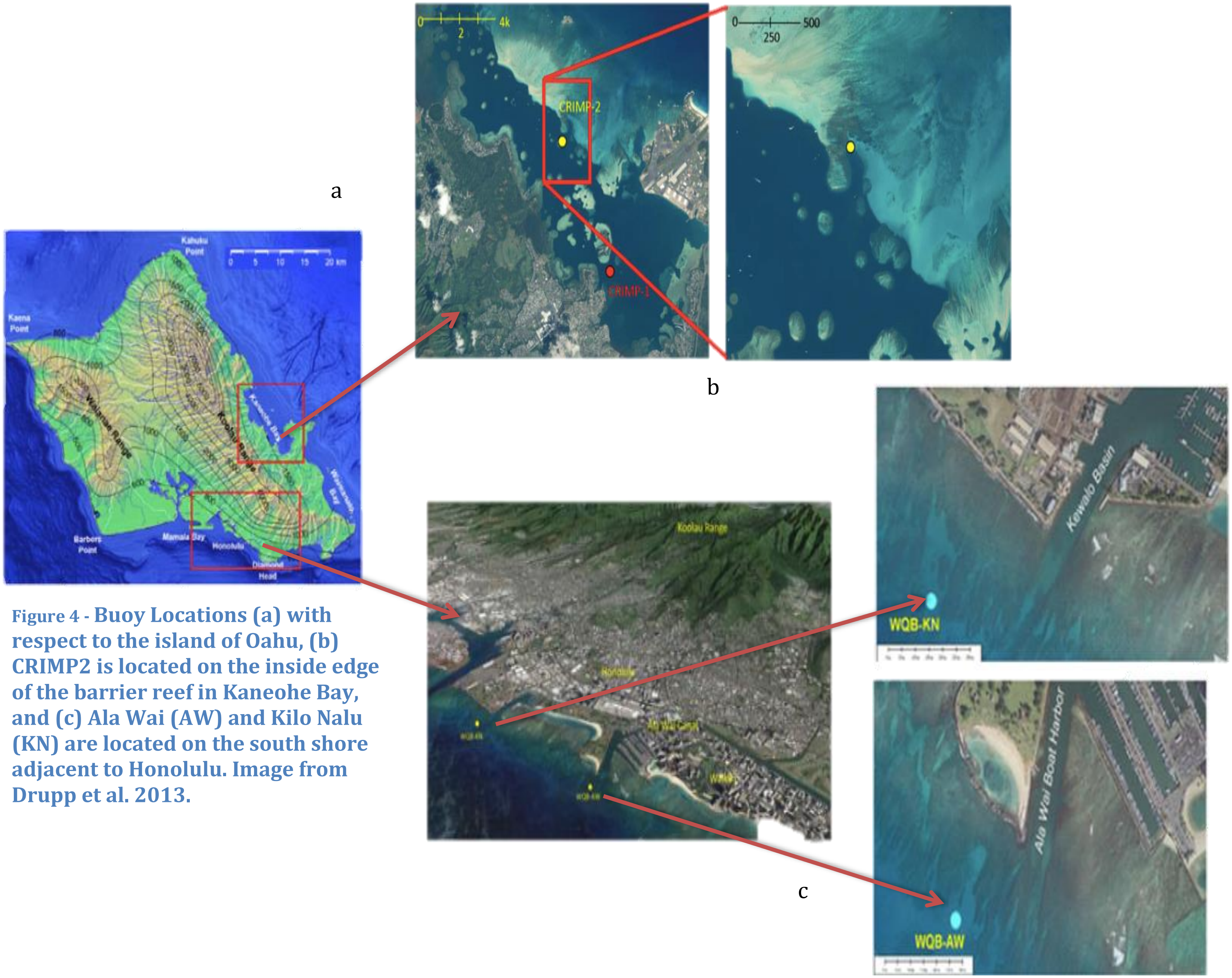

Figure 4 - **Buoy Locations (a) with respect to the island of Oahu, (b) CRIMP2 is located on the inside edge of the barrier reef in Kaneohe Bay, and (c) Ala Wai (AW) and Kilo Nalu (KN) are located on the south shore adjacent to Honolulu. Image from Drupp et al. 2013.**

2.2 DATA AQUISITION

The autonomous pH data were collected using a Satlantic SeaFET ocean pH sensor. The sensing element on the SeaFET is an ion sensitive field effect transistor (ISFET), and the ISFET potential is measured against a reference electrode with a liquid junction and a reference electrode without a liquid junction (Satlantic 2014). Two different ways of potentiometrically obtaining pH measurements provide the ability to monitor the instrument's performance by analyzing the anomaly between the two measurements. The proper functioning of all the equipment and buoy instruments primarily determined the timing and duration of buoy and ancillary equipment deployments. Data that were acquired beginning in 2013 were used for this study, however complete time series data do not exist for the entire time period at any of the three sites. The SeaFET aquired time series data for pH at intervals ranging from 30 minutes to three hours, depending on the perceived needs of each deployment. The Ala Wai pH time series used for this project covers the time periods from January 23 - May 15, 2013, April 22 – July 23, 2014, and October 8 – February 5, 2015. The Kilo Nalu pH time series spans from November 5, 2014 – January 24, 2015, and finally, the CRIMP2 dataset spans from February 25 – May 8, 2013, April 15 – September 9, 2014, and November 24, 2014 – January 26, 2015 (see Figure 5; datasets may be acquired from the Eric De Carlo OA research lab at the University of Hawaii at Manoa).

2.3 TIMESERIES ANALYSIS

The pH time series data were analyzed by comparing and interpreting variations in pH between the two electrodes of each SeaFET, variations at each site over different time periods, as well as comparing differences in the natural environment between sites that could lead to differences in biogeochemical processes. Correlations of pH with other environmental data collected at each of the buoys were also evaluated and compared between the three locations.

Variations in daily and seasonal pH at each of the locations were analyzed primarily by determining the timing of daily peak (high pH) and trough (low) pH measurements. The most frequently occurring daily peak times and trough times observed over one month's worth of data in the winter were compared with the most frequently observed peak times over one month's worth of data in the summer, when available, for each site. In addition, the median and the range of peak and trough times were also calculated and compared between sites.

Dissolved oxygen (DO) and chlorophyll (chl-a) are important parameters measured by the instruments on each of the buoys because they are indicators of biological activity. The strength of correlations between DO, chl-a, and pH was evaluated on daily and seasonal timescales. The DO and chl-a measurements were collected at varying times ranging from every twenty minutes to every hour, however, pH and DO or chl-a measurements were often not taken simultaneously because the buoys measure chlorophyll and DO around 10 minutes after pH, depending on the settings. If a DO or chl-a measurement was collected within a few minutes of a pH measurement, the two measurements were aligned for analysis purposes. However, if a pH measurement was made in between two DO or chl-a points, the two were averaged and then the interpolated DO or chl-a data point was aligned with the pH measurement.

Another important parameter that was evaluated for a correlation with pH is turbidity because it can often be used as an indication of land runoff. The strength of the correlation between turbidity and pH was also compared between each of the sites and different times of the year, similarly to DO and chl-a. Additionally, rain events were identified based on stage height data from two USGS stream gauges located in watersheds that flow into the Ala Wai Canal, one at Waiakeakua and the other at the Manoa-Palolo drainage canal. Spikes in discharge were used to identify the timing and duration of rain events, which were then identified in the pH time series at the Ala Wai site. Correlations were evaluated during these time periods for turbidity, DO, and chl-a to examine the influence of rainfall and to determine if the correlations are stronger when there are rain events than during periods of no rain.

2.4 THE pH SPECTROPHOTOMETRIC METHOD

The pH of seawater samples was measured following the SOP 6b spectrophotometric pH method laid out by Dickson et al. (2009). A 10cm spectrophotometric glass cell was used to contain the sample. An Ocean Optics HL-2000 halogen light source was used and connected via fiber optic cable to the sample cell casing and the spectrometer. Samples were analyzed within a couple of hours after collection after being placed in a 25°C water bath for a minimum of 30 minutes in order to minimize error from changes in the pH of seawater in the sample bottle over time. The blank cell with sample water was then placed in the optic path of the temperature-controlled spectrophotometer for five minutes to ensure a consistent temperature before zeroing the spectrophotometer. After zeroing, 5 μL of m-cresol purple dye was added to the sample in the sample cell and allowed five minutes to equilibrate. The measurements of absorbance at 434, 578, and 730 nm wavelengths were recorded. These are wavelengths characteristic of the dissociated and undissociated dye and a background wavelength that is not absorbed at all. The readings were used to calculate the pH based on several equations.

For the indicator dye used, m-cresol purple, the second dissociation is important,

$$\mathrm{HI^{-}(aq) = H^{+}(aq) + I^{2-}(aq)}$$

Eq. 3

where the various forms of I represent the indicator dye species. The Beer-Lambert Law can relate the measured absorbance at a specific wavelength, λ, to the concentration of the given species as described by equation 4:

$$\frac{A_\lambda}{l} = \varepsilon_\lambda(\mathrm{HI^-})[\mathrm{HI^-}] + \varepsilon_\lambda(\mathrm{I^{2-}})[\mathrm{I^{2-}}] + B_\lambda + e$$

Eq. 4

where B_λ corresponds to the background absorbance of the sample, ε is the molar absorptivity of a given species at wavelength λ, l is the path length, and e is a correction term from the instrument. The pH of the dye and seawater is then calculated using equation 5:

$$\mathrm{pH} = \mathrm{p}K_2 + \log_{10}\left(\frac{A_1/A_2 - \varepsilon_1(\mathrm{HI^-})/\varepsilon_2(\mathrm{HI^-})}{\varepsilon_1(\mathrm{I^{2-}})/\varepsilon_2(\mathrm{HI^-}) - (A_1/A_2)\varepsilon_2(\mathrm{I^{2-}})/\varepsilon_2(\mathrm{HI^-})}\right)$$

Eq. 5

where $\mathrm{p}K_2$ is the acid dissociation constant for the species $\mathrm{HI^-}$ and A_1 and A_2 are the corrected absorbances measured at the wavelengths corresponding to the absorbance maxima of the base and acid forms of the indicator dye, respectively. The various molar absorbtivity terms ε correspond to values measured for the specified species at wavelengths $\lambda1$ = 578 nm and $\lambda2$ = 434 nm, respectively. The value for $\varepsilon_1(\mathrm{HI^-})/\ \varepsilon_2(\mathrm{HI^-}) = 0.00691$, $\varepsilon_1(\mathrm{I^{2-}})/\ \varepsilon_2(\mathrm{HI^-}) = 2.2220$, and $\varepsilon_2(\mathrm{I^{2-}})/\ \varepsilon_2(\mathrm{HI^-}) = 0.1331$. After the pH of a sample was calculated it should then be compared to the measurement taken by the SeaFET at the same time and location. Using the lab pH measurement of multiple samples collected at different times, the anomaly and correction factor were calculated for each SeaFET to evaluate the overall reliability of the time series data using only the factory instrument (SeaFET) calibration function. The relationship between lab pH and SeaFET pH could then be used to correct the time series data and allow more reliable evaluation of how field pH changes respond to various forcing mechanisms.

3.0 RESULTS AND DISCUSSION

3.1 EVALUATION OF TIME SERIES DATA

The reliability of the operation of the SeaFET instrument can be evaluated by observing the pH anomaly between the internal and external pH sensors ($pH_{INT} – pH_{EXT}$). Significant changes in the anomaly over time, which were observed visually in the time series plot, can be used to generalize instrument performance and help quality control measurements. An example of this is shown in figure 5 below,

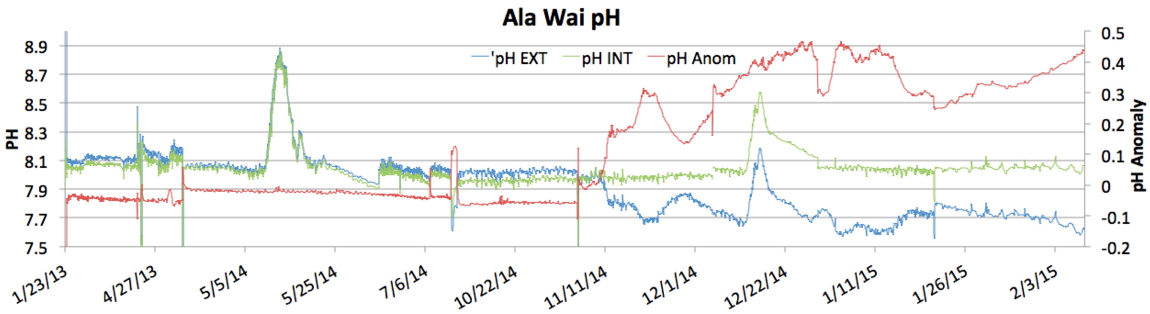

a

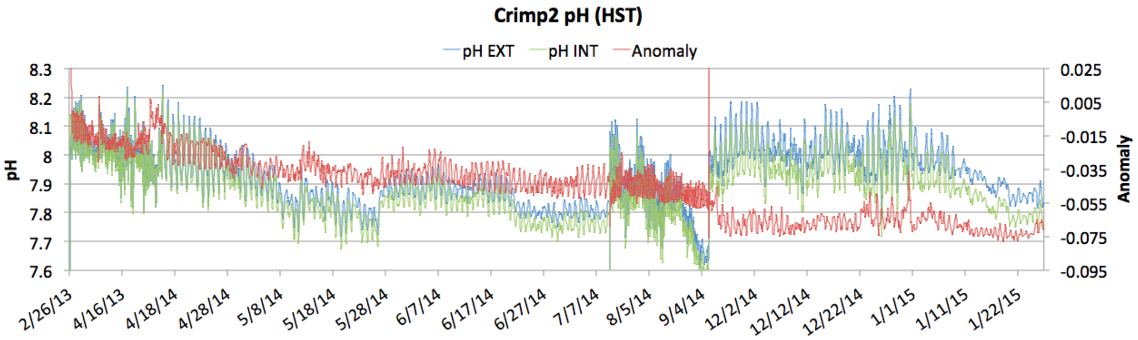

b

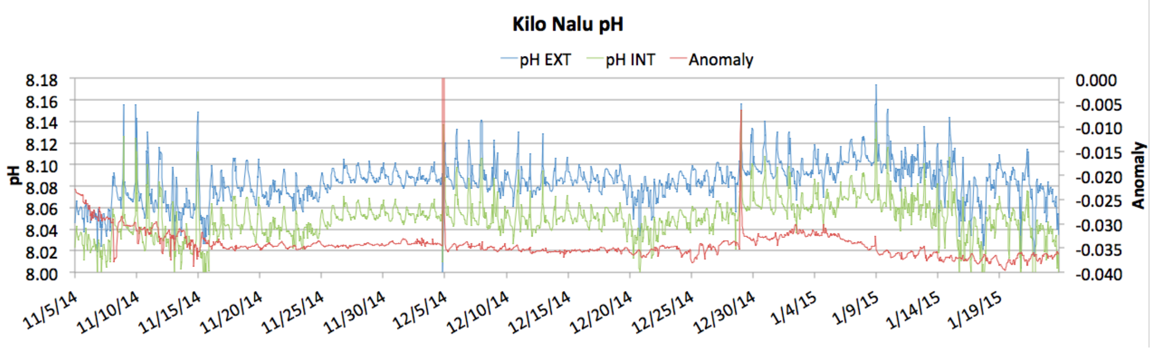

c

Figure 5 - connected time series data sets for Ala Wai (a), Crimp2(b), and Kilo Nalu(c). The external and internal measurements collected by the SeaFET are indicated by blue and green lines, respectively. The difference between these two data sets is the anomaly, represented by a red line. The anomaly can be useful for identifying time spans during which instrument performance was poor and the data may be unreliable. If there is a large difference between the two sensors or if the anomaly is inconsistent or if the anomaly varies with time, measurements should be viewed with suspicion and verified further.

3.1.1 ALA WAI

The anomaly for the entire Ala Wai timeseries falls within the range of -0.1 to 0.5. The anomaly is relatively consistent for the data from January 23, 2013-November 5, 2014, with a value around -0.03. For the time series data collected after November 5, however, the anomaly increases, and the data becomes less reliable and should be considered to have a significant error, at least for one (external) of the electrodes. For OA research, changes in pH on the order of +/- 0.002 can be important, so a large anomaly reaching 0.5 is certainly unacceptable. However, the anomaly increases at a relatively constant rate for much of the period from December 5-27, 2014, and January 24-February 5, 2015, so spikes in pH at Ala Wai, while perhaps not as accurate as desired, still generally portray useful information.

3.1.2 CRIMP2

The anomaly for CRIMP-2 has a range of 0.07, falling within -0.075 and -0.005 (negative values indicate pH_{EXT} is greater that pH_{INT}), which is a much smaller range than Ala Wai. The small difference between the two sensors is an indication that they are working properly (see Figure 5).

3.1.3 KILO NALU

The anomaly ranges within approximately 0.01, from -0.04- -0.03, with the exception of the first half of November 2014. The range is smaller than displayed by both SeaFET deployed at Ala Wai and CRIMP2. Sharp decreases in the anomaly between the two sensors early in any given deployment are an indication that data were collected by the SeaFET without adequate pre-equilibration in seawater. In Figure 5c these sharp decreases can be clearly observed on 12/5/14 and 12/29/14.

3.2 DIURNAL AND SEASONAL VARIABILITY

3.2.1 DIURNAL

The pH of seawater varies over time due to a variety of both natural environmental and anthropogenic factors. Diurnal cycles during which pH increases smoothly to a peak then decreases to a minimum, or a “trough”, are primarily driven by photosynthesis and respiration. The most common time at which the pH peaked generally occurred in the late afternoon, however the time was highly variable at each of the three sites. The time at which pH was lowest (the “troughs”) occurred in the early morning just before the sunrise (see Table 1), although this time was highly variable as well due to a variety of environmental factors discussed later in this thesis.

	RAINY SEASON						DRY SEASON			
	AW Feb '14		**C2 Dec '14**		**KN Dec '14**		**AW Oct '14**		**C2 June '14**	
Peaks										
Mean		8.122		8.114		8.109		8.040		7.896
Median	5:01:00 PM	8.128	4:00:00 PM	8.115	1:01:00 PM	8.102	5:30:00 PM	8.040	8:00:00 PM	7.910
Mode	5:01:00 PM		4:00:00 PM		1:01:00 PM		4:00:00 PM		9:00:00 PM	
Minimum	2:01:00 AM	8.089	12:00:00 AM	8.019	11:01:00 AM	8.087	8:00:00 AM	8.012	1:00 AM	7.808
Maximum	11:01:00 PM	8.149	11:00:00 PM	8.232	11:01:00 PM	8.157	11:00:00 PM	8.058	11:00:00 PM	7.970
Troughs										
Mean		8.091		7.936		8.071		7.986		7.822
Median	8:01:00 AM	8.100	6:00:00 AM	7.940	6:01:00 AM	8.076	6:00:00 AM	7.989	11:00:00 AM	7.832
Mode	11:01:00 AM		3:00:00 AM		7:01:00 AM		6:00:00 AM		11:00:00 AM	
Minimum	5:01:00 AM	8.044	12:00:00 AM	7.775	1:01:00 AM	7.999	1:00:00 AM	7.947	10:00 AM	7.749
Maximum	2:01:00 PM	8.116	10:00:00 PM	8.001	6:01:00 PM	8.091	1:00:00 PM	8.017	3:00 PM	7.873

Table 1 – Summary pH peak and trough data for selected wet and dry season months. The columns classify the buoy location and month in which data were used. The left three columns are rainy season months and the right two are dry season months. The top half of the table summarizes the average time of day at which pH peaked for that month, the average peak value, the median time and value, the most commonly occurring peak time (mode), the earliest time and minimum pH peak value, and the latest time and maximum value. The same statistics are given in the bottom half of the table, but for daily low pH times and values, or "troughs".

3.2.2 SEASONAL

The median peak times for selected months are illustrated in Figure 7. Data from this project reveal evidence for wet and dry seasonal differences in pH peak times. This is likely due to the length of day. All locations have large ranges of times at which pH peaks during the day, so there are likely different factors influencing production in the different areas besides sunlight. At CRIMP2, the median pH peak time occurred at 8pm in the summer month of June, and is four hours earlier at 4pm in the rainy month of December (see Figure 7). Resent research has also been trying to determine reasons for very late (albeit smaller) peaks in pH that occur late at night (see Figure 6). It has been speculated that this is due to biological processes and related to coralline algae, but the actual process and mechanism are still not fully understood. There may be additional processes occurring other than photosynthesis driven by visible light (Calhoun 2016).

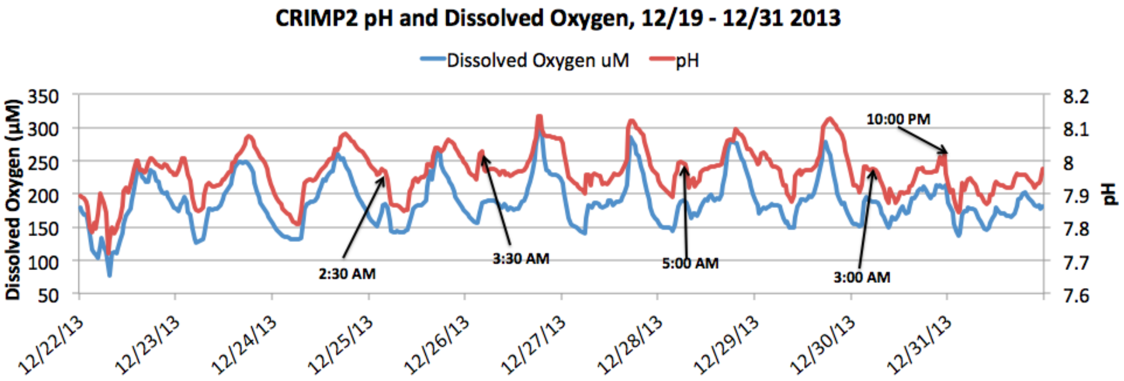

Figure 6 – Plot of pH and dissolved oxygen showing late peak pH times, which are a common occurrence. These late peak times are relatively consistent, suggesting a well-timed process is taking place. However, reasons for this phenomenon are still not completely understood.

At Ala Wai, the median peak pH time occurred at 5:30 pm during the dry month of October, and shifted back to 5:00pm during the month of February. However there are similar day lengths during these two months, so a significant difference in peak time is not expected. There were no available data in the summer for comparison at Kilo Nalu, however, the median peak time in December 2014 at Kilo Nalu was 1 pm. This time is considerably earlier than the wet season peak times at the other two sites. Lower rates of photosynthesis and a much smaller range of pH values observed at this location may lead to a much noisier pH record and may cause erroneous identification of a much earlier peak time.

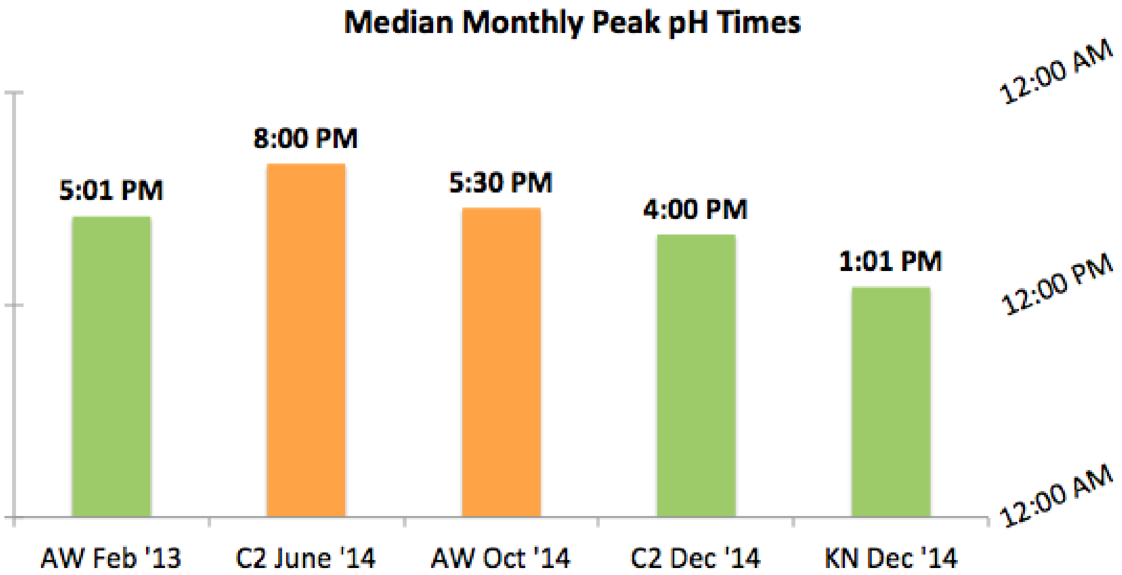

Figure 7 – Median times for peak pH for selected wet season (green) and dry season (orange) months. The summer months generally have later peak pH times, while the winter season months generally have earlier peak times.

3.3 CORRELATIONS OF pH WITH OTHER ENVIROMENTAL PARAMETERS

3.3.1 DISSOLVED OXYGEN

The dissolved oxygen content of seawater is closely tied to the pH in the three buoy locations. This is illustrated in Figure 8, showing approximately two weeks of pH and dissolved oxygen data. At Kilo Nalu, however, dissolved oxygen appears to lag the pH at certain times (e.g. from 11/27 – 11/30 2014; see Figure 8). The strength of the correlation between dissolved oxygen and pH is strongest at CRIMP2 and weakest at Kilo Nalu with R^2 values of 0.67, 0.81, and 0.28 at Ala Wai, CRIMP2, and Kilo Nalu, respectively (See Figure 9).

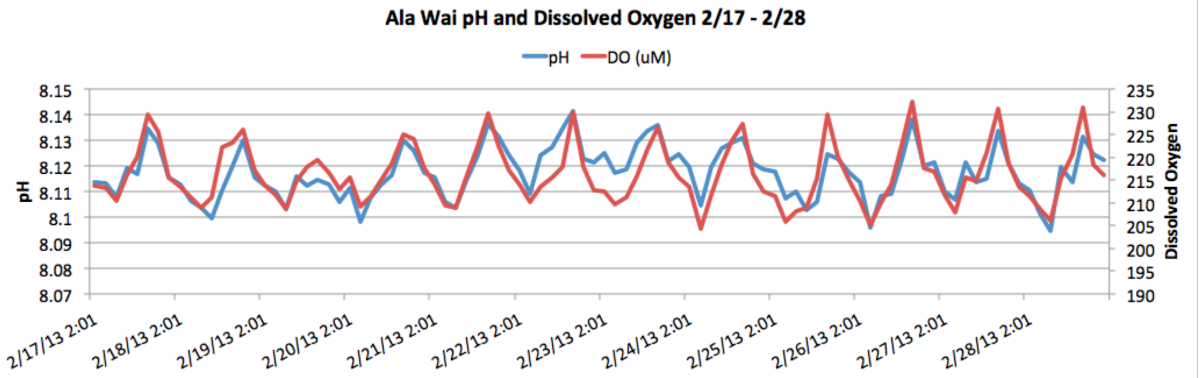

(a)

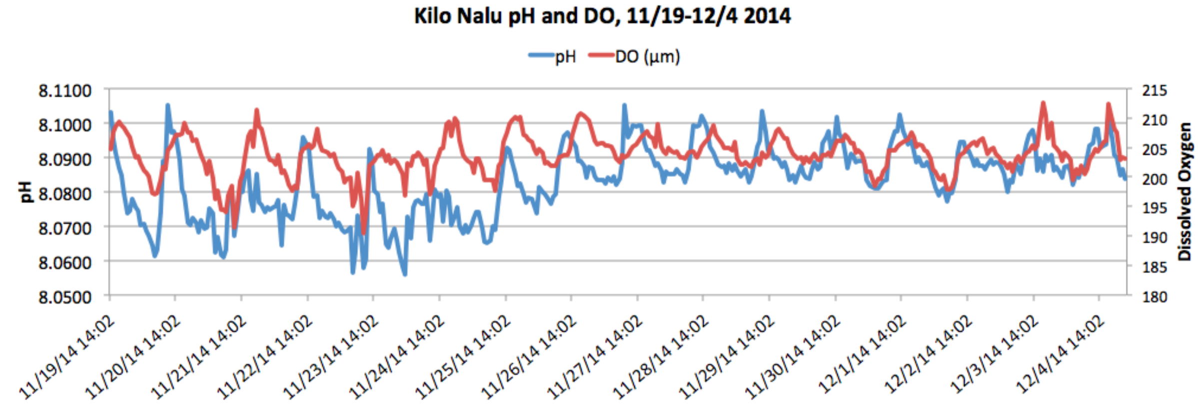

(b)

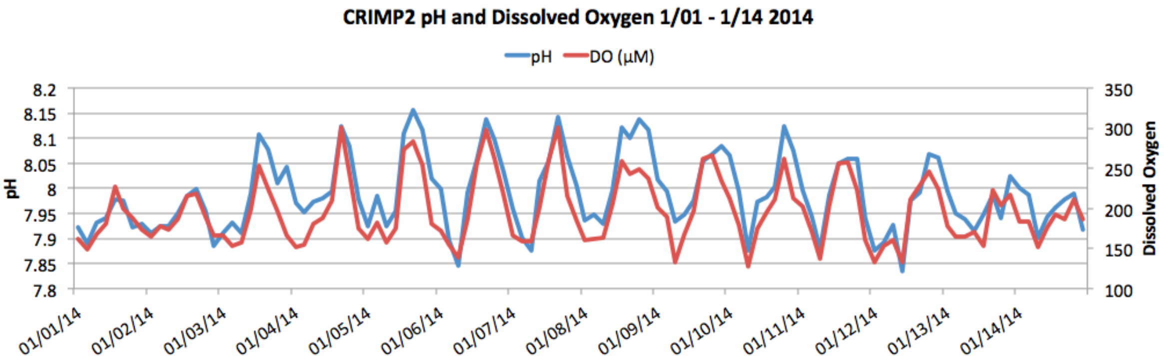

(c)

Figure 8 - Dissolved oxygen and pH plots for (a) Ala Wai, (b) Kilo Nalu, and (c) CRIMP2. Note the difference in scales. The daily range in DO for CRIMP2 is extremely large, spanning from 150 µM to 300 µM, while Kilo Nalu and Ala Wai only have a daily DO range of about 20 µM. Note the difference in pH scales as well. The peak and especially trough values are generally lower for CRIMP2 and higher for Ala Wai, however the range is larger for CRIMP2, similar to the dissolved oxygen.

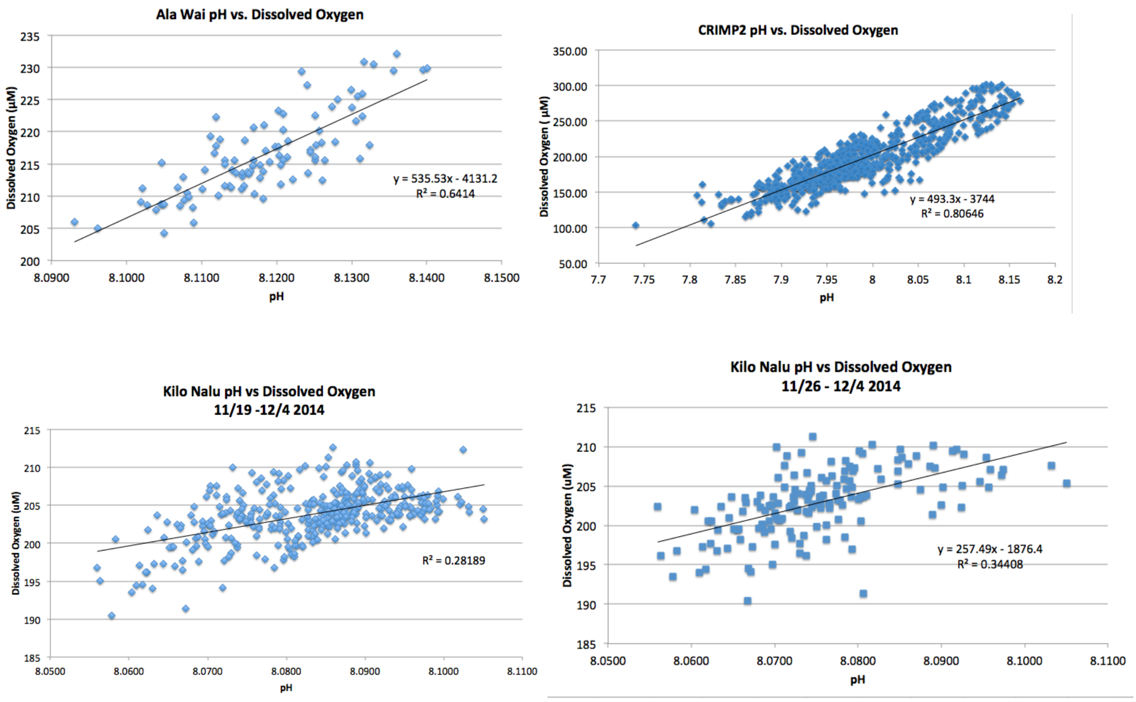

Figure 9 - Correlations between pH and dissolved oxygen for (a) Ala Wai, (b) CRIMP2, (c) Kilo Nalu for the same time periods used in figure 8. There may be be two separate correlations for Kilo Nalu during this time period. Figure 8d includes only data starting after when the dissolved oxygen data slightly lags the pH, and the correlation is slightly stronger yet does not reach those observed for Ala Wai or CRIMP2.

3.3.2 TURBIDITY

Turbidity did not exhibit a strong, if any, correlation with pH. In fact, there was no correlation between pH and turbidity at Kilo Nalu, and only smaller clusters of turbidity data correlated with pH among the January-May 2013 data set at Ala Wai. When the data were divided according to the SeaFET instrument number (17 and 18), however, and data from SeaFET 18 were further divided based on three separate deployments, stronger correlations were exhibited. Yet, while set 18A and 18B had unexpected negative correlations, data from SeaFET 17 showed a weak positive correlation (See Table 2, Figure 10). When there is a negative correlation such as for datasets 18A and 18B, the pH appears to be more strongly influenced by freshwater effluent from the Ala Wai Canal although the turbidity of this riverine water remains rather low (i.e. < 9.5 NTU). So when there is a stronger correlation during certain times, it likely reflects changing contents of discharged water, as freshwater has a lower pH than seawater and the freshwater flux is greatest at Ala Wai during periods of high rainfall when turbidity is also likely to be higher.

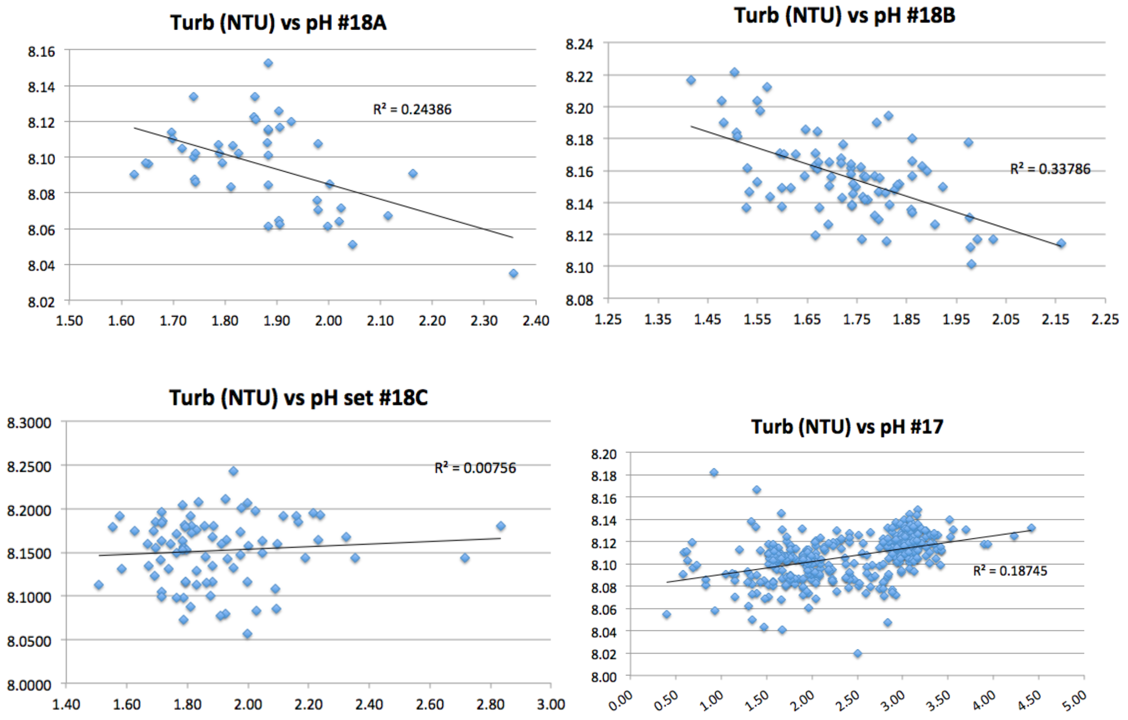

Figure 10 - Correlations with turbidity at Ala Wai. Different correlations were observed during specific time periods, such as in data sets 18A and 18B. However there was not a strong correlation between pH and Turbidity overall.

Ala Wai Turbidity and pH Correlation

Data Set/Instrument Number	Time Period	R^2
17	1/31/13 – 3/21/13	0.187
18A	4/29/13 – 5/4/13	0.244
18B	4/19/13 – 4/29/13	0.338
18C	5/4/13 – 5/15/13	0.008

Table 2 - Strength of correlations between pH and Turbidity at Ala Wai over four different time periods. To check for potential offsets caused by different instruments, SeaFET 17 was separated. Then different clusters of data (from SeaFET 18) were separated into A, B, and C, to look for stronger correlations.

On short term (daily scales), the turbidity time series follows the pH trend poorly at Ala Wai. There is a longer-term slight increase in pH from approximately 2/8 – 2/12 2014 that corresponds to a slight increase in turbidity over approximately the same time period (See Figure 11a). This relationship appears relatively weak, however, the longer-term relationship of pH to chlorophyll is slightly stronger (see Figure 12). This indicates that turbidity alone does not control production, hence does not control the pH. The pH varies inversely with turbidity much more closely at Kilo Nalu, however many of the trends in turbidity lag the similar trends in pH by approximately six hours for much of the time period from 11/15 – 12/3/ 2014 (See Figure 11b). This may be due to the relatively small range of values measured at the location, leading to a noisier pH record, however the cause of this lag remains unclear.

It is important to note the significant differences in turbidity ranges between the two south shore sites. Ala Wai has a range of about 4 NTU from 1/31 – 3/18 2013, while Kilo Nalu only has a range of approximately 0.7. The values at Kio Nalu are also much smaller, so more prone to instrument error, which may be the reason why there is a poor correlation with pH, and perhaps with dissolved oxygen as well.

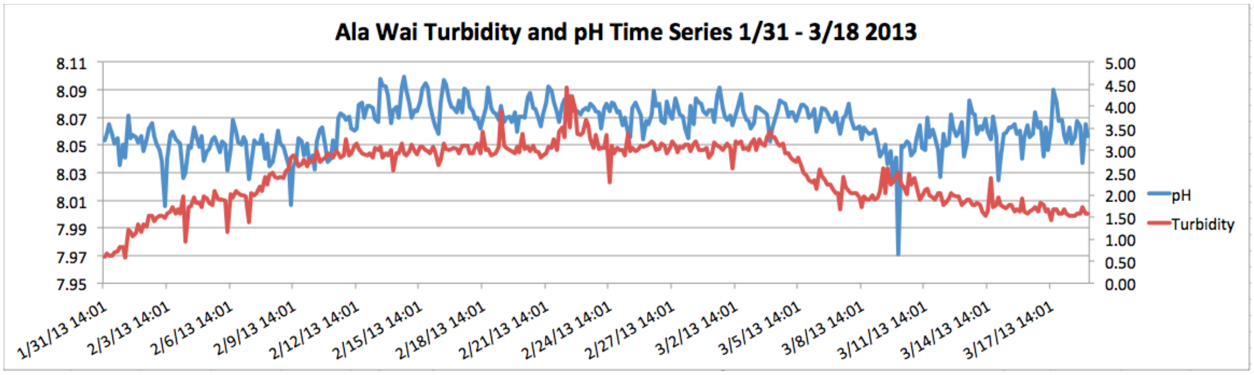

a

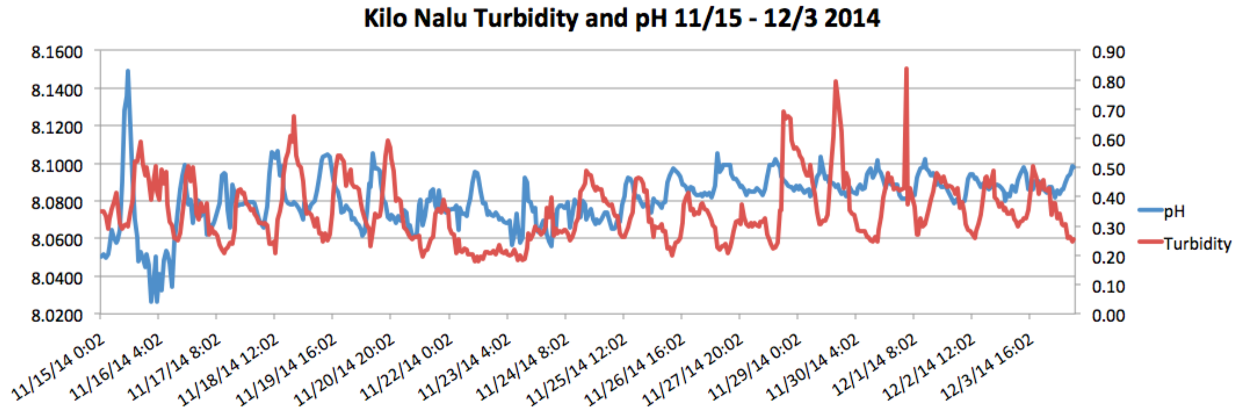

b

Figure 11 - Turbidity with pH plots for Ala Wai and Kilo Nalu. Note the large difference in turbidity scales.

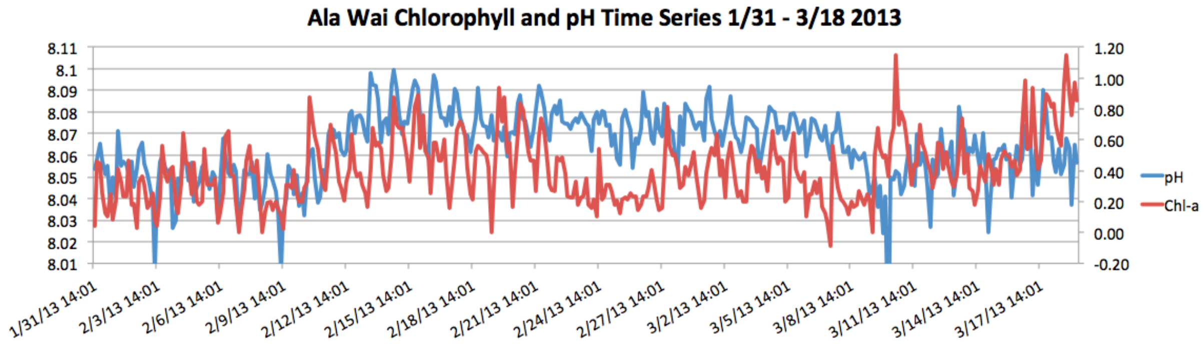

Figure 12 – Chlorophyll and pH plots for at Ala Wai. The general trends of chlorophyll seem to loosely follow those of pH

3.4 INFLUENCE OF RAINFALL

3.4.1 INFLUENCE OF RAIN EVENTS ON BIOGEOCHEMICAL PROPERTIES

Two USGS stream gauges were used to obtain discharge data for this project (See Figure 13). Both gauges at Waiakeakua and Mano-Palolo Drainage Canal at Moilili measured a considerable increase in discharge, indicating two rain events and increased discharge from the Ala Wai Canal, during the time period from February 18 to March 23, 2013. The first event occurred over nearly three days from approximately 12:00 am on 2/21 to 8:00pm on 2/23/2013, and the second lasted only about 24 hours, from approximately 11:00pm on 3/9 to 11:00pm on 3/10/2013 (See Figure 14).

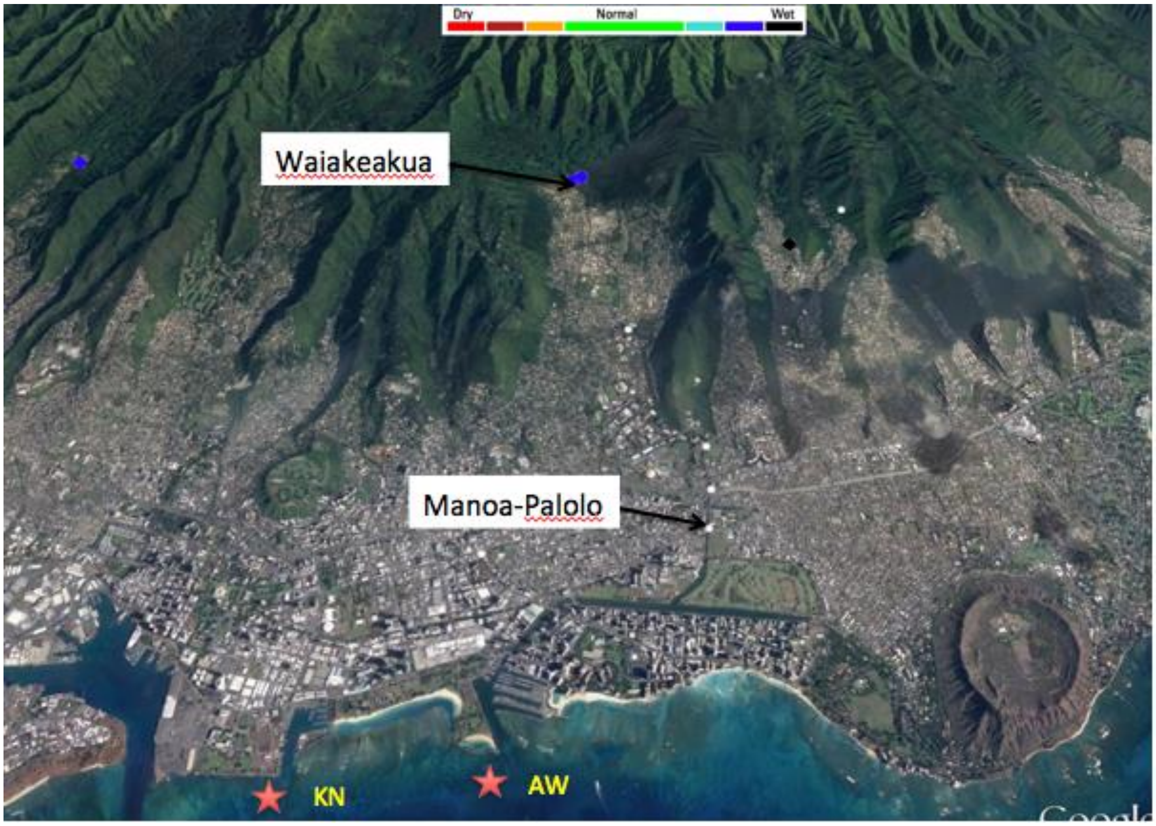

Figure 13 – Stream gauge locations used to determine rain events

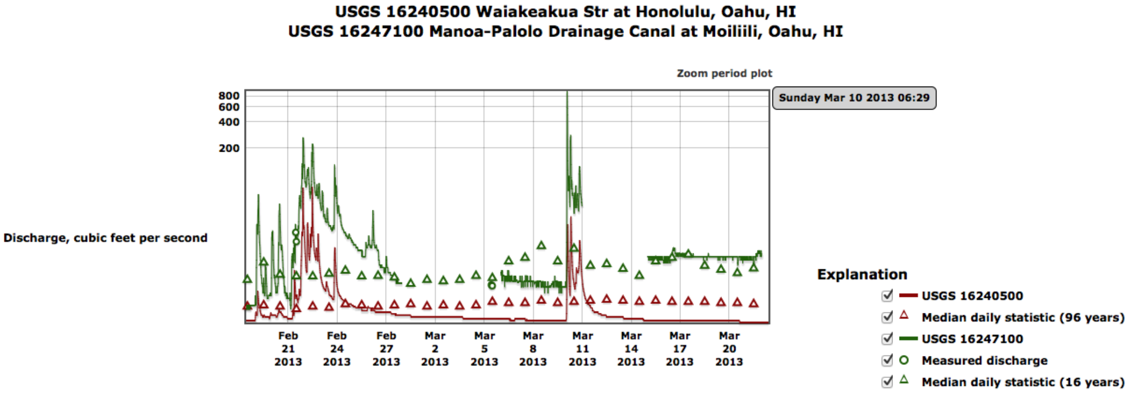

Figure 14 - Waiakeakua (red) and Manoa-Palolo (green) USGS stream gauges showing discharge. This plot was used to determine the time period in which rain events occurred.

An influence from rainfall on pH was not readily apparent at Kilo Nalu, however there was an observable change in pH, as well as in turbidity and chlorophyll, at Ala Wai (See Figure 14). However, contrasting changes in pH occurred at Ala Wai during these two major rain events spanning the period of approximately one-month (2/18/13 – 3/23/13). During the first rain event pH at Ala Wai reached a high of 8.14, with a general, slightly increasing trend throughout the event. In contrast, during the second rain event, the pH decreased quite sharply, reaching its lowest point of 8.02 during the overall period from 2/18 – 3/23 2013. Dissolved oxygen followed the same trends as pH, which is expected if photosynthetic activity and respiration govern, as discussed previously (See Figure 8a).

Salinity is the parameter that most strongly provides evidence for rain events. During the rain events mentioned above, large decreases in salinity were observed, consistent with inputs of freshwater from runoff in the Ala Wai Canal. The salinity dropped to nearly 34.2 during the first rain event and nearly 34.4 within a day after the second rain event from a baseline salinity in the range of 35.2 – 35.3 (See Figure 15). When rainfall data are not available, salinity data can be used as a quantitative proxy for freshwater inputs.

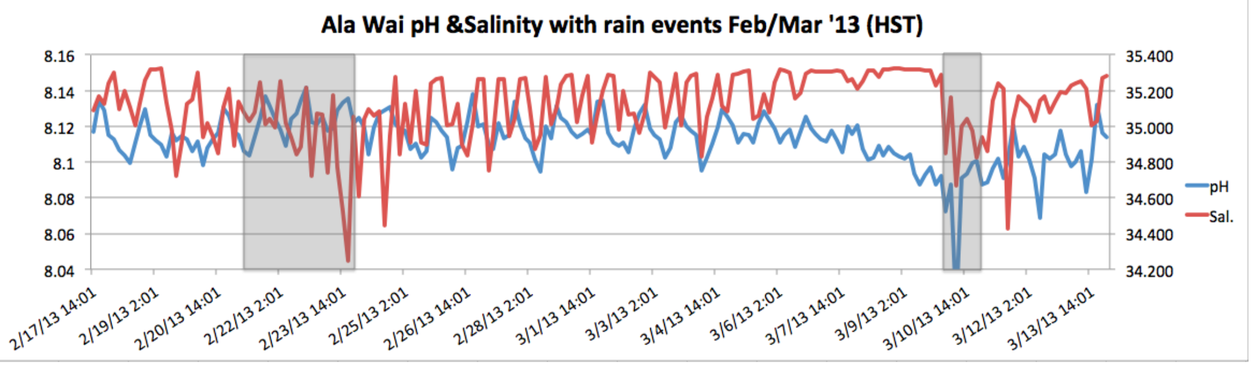

Figure 15 – Salinity and pH with rain events highlighted in grey boxes. Sharp decreases in Salinity are observed after rain events reaching as low as 34.2 when typical values are around 35.0 to 35.2.

Turbidity at the Ala Wai buoy increased during both rain events (Figure 16c) although because this site is approximately 200 m offshore from land and the outflow of the canal, much of the suspended load should have already been deposited. The peak in turbidity, however, was significantly higher during the first event, reaching 4.5 NTU compared to only 2.6 during the second event. Turbidity showed a relatively sharp decrease, reaching its lowest point of this time period, three days prior to the second rain event. When turbidity increases, it was expected that pH would increase as well, however the data shown in Figure 16c gives evidence that this is not always true. This may be related to the antecedent period between the two rain events. While there may have been greater discharge during the second event, perhaps a lot of dirt and pollution that accumulate in runoff and increase the turbidity was “rinsed” off during the first event, which resulted in less turbidity during the second event. Additionally the soil may have been more saturated after the first rain event and rainfall during the second event may have pushed more groundwater, poor in suspended solids, into the streams and Ala Wai. With regard to pH, however, turbidity is not always as useful for predicting trends.

Chlorophyll (Figure 16b) showed little change in trend during the first rain event, however it sharply increased to a peak of 1.15 μg/L in the latter half of the second event, despite the decrease in pH and dissolved oxygen. Based on these observations, chlorophyll is not a reliable indicator of seawater pH trends as at Ala Wai during rain events because of potential inputs of land-based pre-formed chlorophyll.

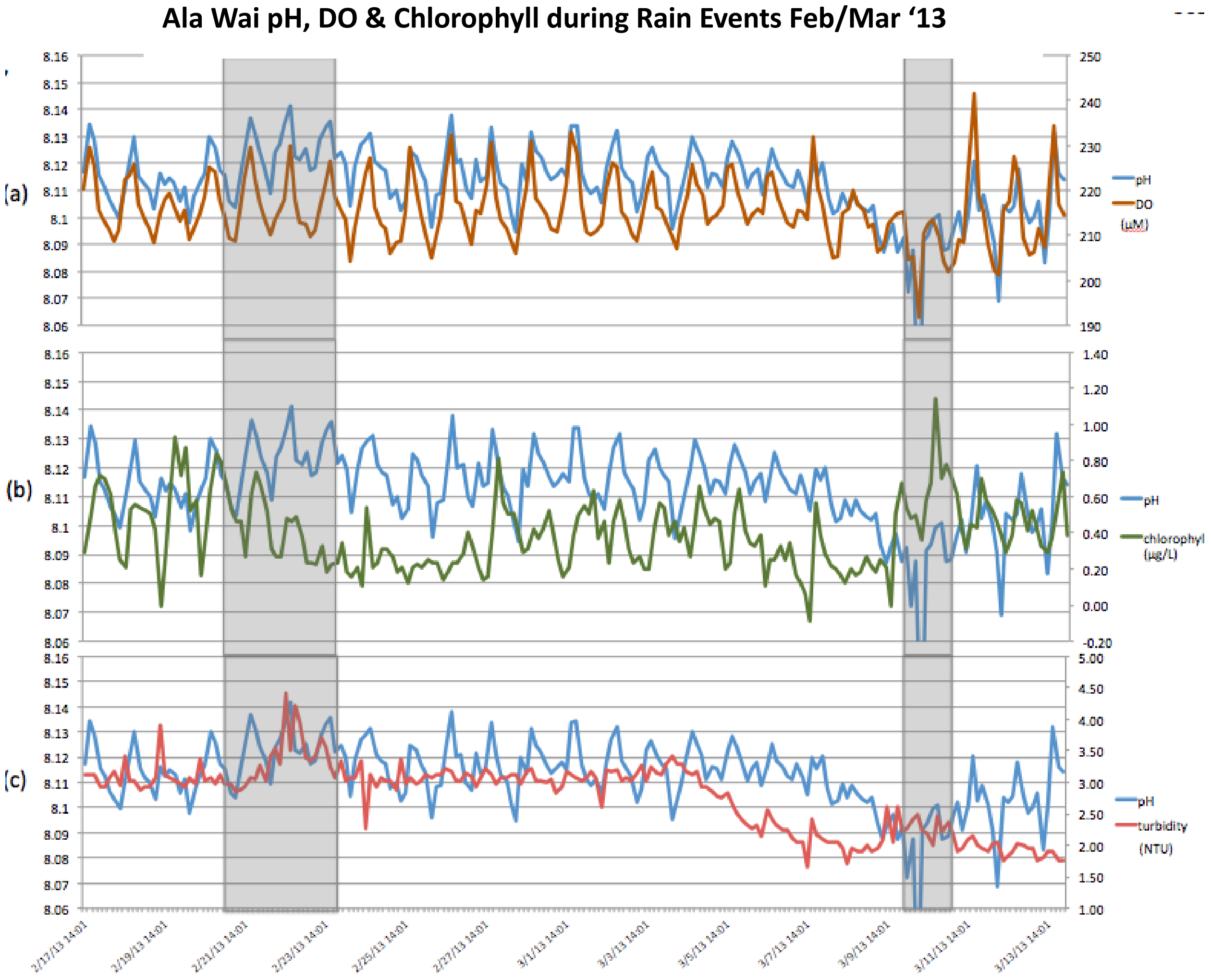

Figure 16 - Plot of pH and (a) dissolved oxygen, (b) chlorophyll, and (c) turbidity, with rain events highlighted in grey. During the first rain event, pH slightly increases, however in the second, pH sharply decreases. The contents in the Ala Wai that reflect or influence production and respiration must therefore be highly variable and control pH, particularly during rain events. More data about the contents of the water in the Ala Wai canal are needed to accurately predict the effect of rainfall on pH.

As mentioned above, salinity can potentially be used as a proxy for rainfall if data for the latter are unavailable. There was most likely a rain event on 1/9/2014 in Kaneohe Bay (See Figure 15), which likely caused the considerable drop in salinity to 34.4 when the typical range at CRIMP2, located well away from any stream inputs, is between 34.6 and 35.4. Rainfall is expected to decrease the pH since rainwater can have a pH as low as 5.6 as it is in equilibrium with atmospheric CO_2. Yet, there was not a very large decrease in pH when salinity decreased sharply. It is possible that there is not very much mixing of rainwater with seawater and the pH below the surface is not influenced significantly by rainfall.

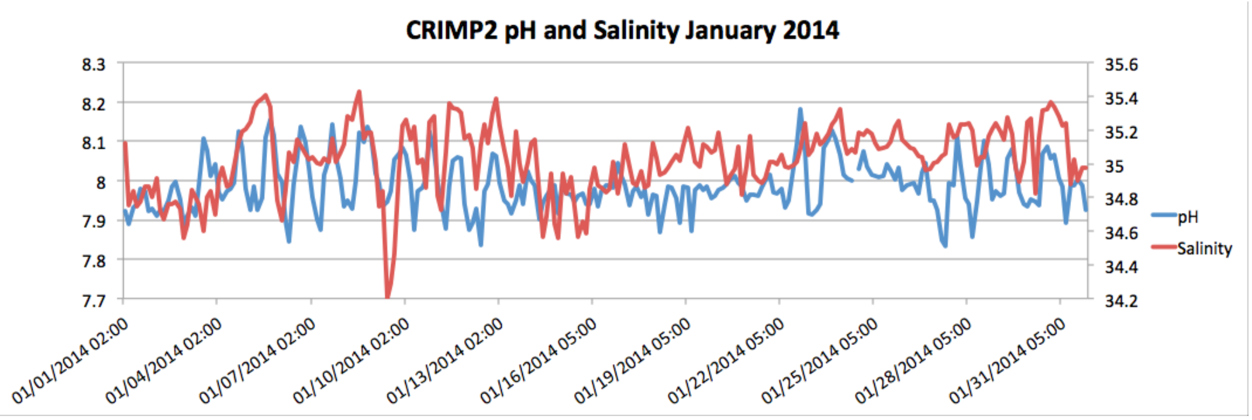

Figure 17 – Plots of pH and salinity at CRIMP2. There was very likely a rain event on 1/9/14, however the pH was expected to decrease as well with the addition of freshwater.

3.7 SPECTROPHOTOMETRIC pH MEASUREMENTS

Analysis of a few samples collected from CRIMP2 indicates a deviation from the SeaFET measurement (7.962) of around -0.2 pH units, which is relatively large (see Table 3). This deviation is expected to be much less now since more accurate and precise measurements have been obtained, and consistency was not yet achieved when these preliminary CRIMP2 measurements were taken.

Sample	pH
CRIMP2 14:00 4/14 #1	7.766469552
CRIMP2 14:00 4/14 #2	7.760458845
CRIMP2 14:00 4/14 #3	7.758375777

Table 3 – Spectrophotometrically measured pH values of a CRIMP2 bottle sample

When the pH of test seawater samples was measured spectrophotometrically in the laboratory, the pH did not stabilize immediately. The first one or two samples typically showed pH that was about 0.1 units lower than the measurements made subsequently (see Figure 18). Therefore, when making spectrophotometric pH measurements, at least three junk seawater samples should be measured initially in order to ensure subsequent accurate results. A standard deviation of 0.007 was obtained from 12 measurements after removing the first measurement (see Figure 18). To confirm the accuracy of the method, reference material with a pH of 7.8796 was measured, and the spectrophotometric method measured the sample to be 7.8703.

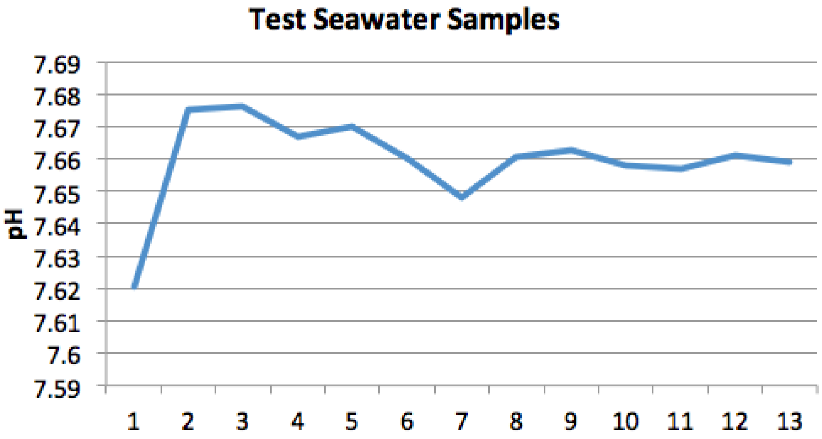

Figure 18- Plot of measurements made with junk seawater samples. Typically the first 1-3 samples are low before the measurements become more consistent.

Sample	pH
Test #1	7.62045227
Test #2	7.675041753
Test #3	7.676346382
Test #4	7.667036006
Test #5	7.669833453
Test #6	7.660073097
Test #7	7.64794958
Test #8	7.660519315
Test #9	7.662502688
Test #10	7.658003269
Test #11	7.656783009

Test #12	7.660991625
Test #13	7.659189269

Table 4 – Spectrophotometrically measured test seawater samples

4.0 GENERAL INTERPERETATIONS

4.1 RELIABILITY OF TIMESERIES DATA

Time series data collected autonomously are useful when they are quantitatively accurate. The accuracy of autonomous data can be evaluated by measuring pH bottle samples spectrophotometrically. Additionally the SeaFET anomaly (i.e. ΔpH between the two electrodes) and identification of any unreasonable values, can also help improve confidence that the pH data are reliable and may be used for further ocean acidification research. Of the nearly twenty months of time series data between the three sites examined in this study, about 75% of the data can be trusted based only on the anomaly between the two SeaFET pH sensors (see Figure 19). All data must be quality controlled for unusual pH changes, which may result from bio-fouling on the instrument's sensors or may be due to some instrument malfunction or other natural phenomenon.

For example, the Ala Wai data collected after 11/5/2014 cannot be confidently used. A very large anomaly develops progressively between the two sensors after November 2014, which reaches 0.4 units (see Figure 19a). This is greater than the entire natural range ever observed at CRIMP2, as well as any change observed in photosynthesis/respiration cycles. The difference between the two sensors should be relatively constant because a 0.4 change in pH say, from 7.8 – 8.2, represents a 60% change in hydrogen ion concentration, [H+]. This change is far beyond any expected change due to OA over the next 100 years. Fortunately, however, comparisons of the

pH_{INT} data from this period to earlier deployments suggest that this electrode was functioning reliably and only the pH_{EXT} electrode was experiencing problems.

It is, however, important to realize that when the anomaly decreases sharply at the beginning of a new deployment, it is because the recently deployed sensors are still equilibrating. Measurements taken within a few hours after deployment are not accurate if the electrodes were not properly acclimated in seawater for enough time before the SeaFET was deployed. Additionally, even when the anomaly does not change significantly, the pH sometimes will vary to unusually high or low values, such as what was measured from 5/8/14 – 6/1/14 at Ala Wai (see figure 19a). During this time period, the pH increased dramatically to a value of 8.9, which is extremely unlikely for seawater, even in very high productivity areas, with a pH range typically not going above about 8.15 (Drupp et al. 2013). This was confirmed after looking at the maintenance report, which reported algae on the sensors, which would have artificially increased DO, and therefore the pH at the surface of the electrodes, whereas the water column did not necessarily experience the same level of productivity.

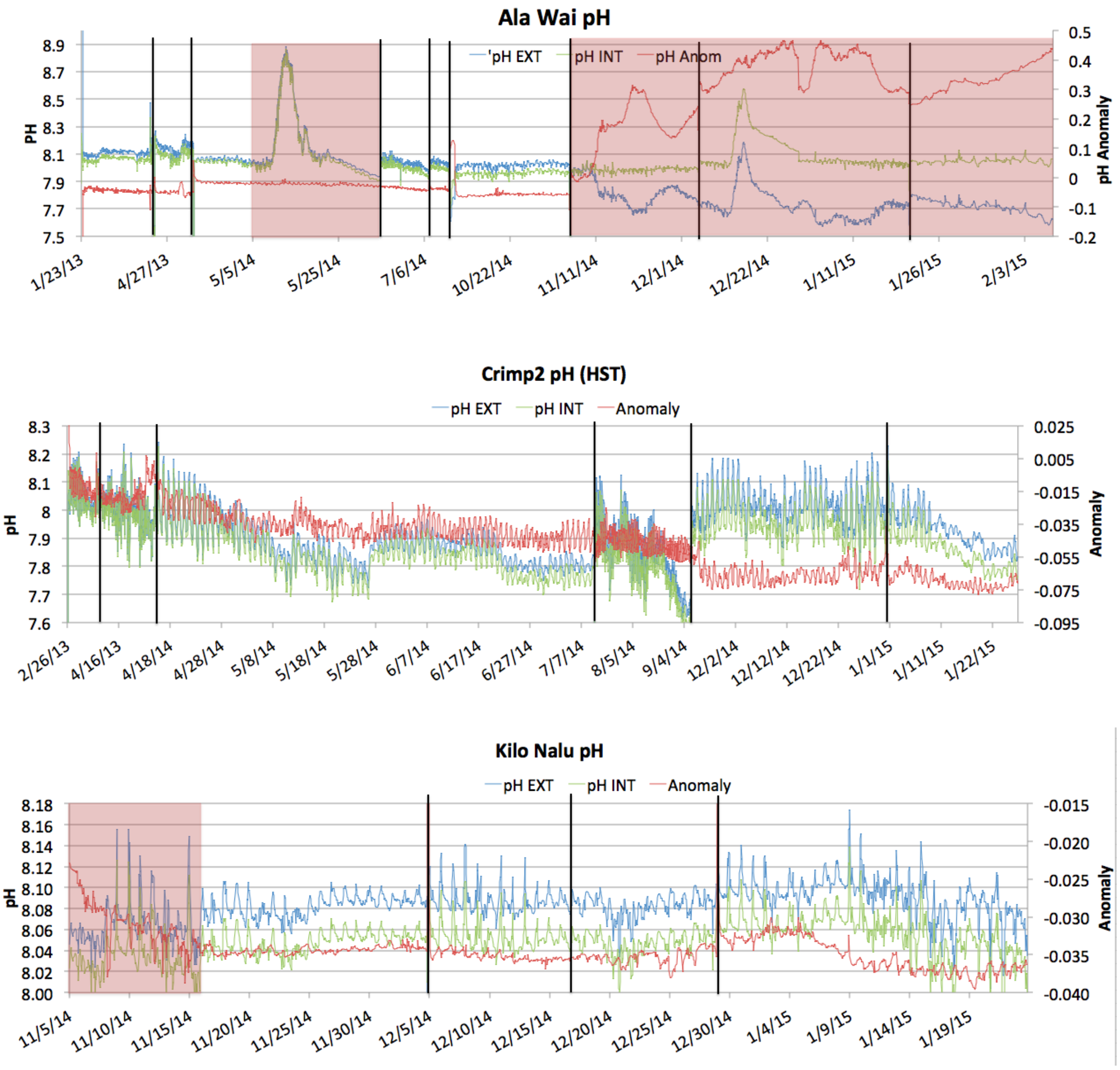

Figure 19 – pH internal (green) and external (blue) timeseries plots with anomaly (red). New deployments are marked with black lines. Bad data based on a large or inconsistent anomaly or unreasonable values, such as pH values reaching 8.9 at the Ala Wai site in May 2014, is highlighted in red. It is very important to note the differences in scales for the anomaly. The anomaly for Ala Wai was often an order of magnitude greater than CRIMP2 or Kilo Nalu.

The second way used to check data accuracy is by comparing measurements made in the laboratory to those measured by the SeaFET at the same time the bottle samples were collected. Ideally, there would be a consistent difference between the pH values measured by the spectrophotometric method and those measured by the SeaFET, and a correction could be made in the future to the time series data that would then improve the accuracy of the sensor data. Water samples from each of the sites will be collected for such a comparison in the next few months.

4.2 DIURNAL VARIABILITY

4.2.1 DISSOLVED OXYGEN AND pH

Dissolved oxygen (DO) may be used as a proxy for pH due to the association of these two parameters through photosynthesis. Of all parameters mentioned in this study, the pH of seawater is most strongly influenced by photosynthesis and respiration in the coastal ocean of Oahu. This is especially evident at the CRIMP2 and Ala Wai sites, where this process exerts the dominant control on water chemistry. The correlation between pH and dissolved oxygen is not as strong at Kilo Nalu as at the other two sites, however, this may result from the small range of values for pH and dissolved oxygen partly owing to the short residence time of seawater at this site and a lack of strong photosynthesis/respiration cycles associated with low nutrient inputs compared to Ala Wai. The daily variability for dissolved oxygen at Kilo Nalu was only about 25% of the daily dissolved oxygen range observed at Ala Wai and less than 10% of the range observed at CRIMP2. Such a small change make it more difficult to detect subtle changes with the equipment used and the frequency at which measurements were collected.

4.2.2 PEAKS AND TROUGHS OF pH

Because pH is most strongly influenced by photosynthesis and respiration, the maximum pH over a 24-hour period should occur when the extent (or rate) of photosynthesis is highest, and a minimum pH will occur when respiration is highest. The pH is therefore expected to peak in the late afternoon and reach a minimum in the early morning before sunrise. The time pH peaks, however, changes to some extent on a day-to-day basis. This may be due to other factors that influence photosynthesis in a given location. Cloud cover likely influences the amount of sunlight reaching the water column, hence photosynthesis, or turbidity from particle input to coastal waters may also have a direct effect on pH, Ala Wai has indicated. This difference in turbidity may also affect the time of peak pH by causing light limitation to primary producers in the water.

4.3 SEASONAL VARIABILITY

As a result of longer days during the summer months, the peak amount of photosynthesis occurs at a later time, in general, than in the winter months. This is what was observed most clearly at CRIMP2 when the median peak time shifted by four hours from 4pm in December to 8pm in June. Since this is a rather late time in the evening after the sun has set, there may also be other factors contributing to late peak pH times. These may be related to a process other than photosynthesis driven by light, possibly related to coralline algae, as recently suggested by Calhoun et al. (2016). Rior work has shown that infrared light can also drive primary productivity. Thus, moonlight may provide enough infrared light to fuel a small amount of photosynthesis after dark. However, late spikes in pH are still being studied and are not yet understood completely.

4.4 INFLUENCE OF RAINFALL

Rainfall events would be expected to cause an increase in pH at locations that are affected by land runoff such as the Ala Wai, since runoff contains nutrients that promote production and use dissolved CO_2. Data, however, suggest that this may not always be the case. Runoff can contain different amounts of various materials from watersheds and urban areas, including sediments and nutrients in addition to freshwater. The nutrients can promote plankton and algae growth in the ocean, which typically is nutrient limited around Hawaii (e.g. Yasunaka 2014). Production then lowers pCO_2 and increases pH. There was, however, a significant drop in pH at the Ala Wai site during one rain event examined in this project, and the reason remains unclear. Turbidity increased slightly, and DO decreased along with pH before subsequently increasing sharply. Chlorophyll is interesting as well because it never drops below about 0.2 µg/L, when it reaches nearly zero at other times during this period. However, it increases very sharply during this rain event. One possible explanation for this could be that because this was a short, intense rain event, input of a lot of dead organic matter or microorganisms in addition to nutrients in the Ala Wai initially led to enhanced respiration, before driving photosynthesis, which spiked shortly thereafter, leading to high chl-a, DO, and pH (see Figure 16).

At CRIMP2, rain events would be expected to cause pH to decrease. Because rainfall is slightly acidic, and CRIMP2 is too far offshore to be influenced by land runoff under most conditions, rain should cause a decrease in pH. However, the salinity data, which should reflect rainfall, did not show any corresponding drops. One possible explanation could be a lack of mixing of rainfall deeper into the water column, and the pH, which is measured at 0.5-1 m below the surface, was not greatly influenced by rain at this depth.

5.0 CONCLUSIONS

Ocean acidification is a growing concern among scientists based on its potentially harmful effects on a variety of marine organisms and coral reef ecosystems. It is very important to obtain measurements of pH that are as accurate as possible because while variability in pH is relatively large on seasonal or daily timescales, very small annual changes in pH are difficult to measure. Additionally, long-term changes in pCO_2 are important because of the potential sensitivity of organisms to relatively small changes in the carbon system. The spectrophotometric method of measuring pH can be used as an additional tool to verify the accuracy of time series measurements taken by instruments such as the SeaFET and calibrate them, and as a measurement to use to obtain other carbon system parameters such as dissolved inorganic carbon (DIC) and total alkalinity (TA) if one of these other parameters is known as well.

There are several important insights gained after analyzing the coastal Oahu pH data in this project. Based on the parameters determined for this project in relation to pH measurements, it appears that the processes of photosynthesis and respiration exert a dominating influence on the pH of seawater around coastal Oahu rather than OA. Dissolved oxygen, a product of production in the water column, may even be used as a proxy for pH for general analysis when pH data are unavailable. Due to biological production's control on the pH of seawater and the extensive influence humans have on Oahu's coastal environment, it is important that runoff and wastewater discharge are managed properly as to not disturb sensitive ecosystems, such as coral reefs, in coastal zones. The Ala Wai is an important example of how large of an effect urban rainwater discharge can have on seawater pH. Obtaining high quality pH data and observing patterns and variability in pH now will be useful when tracking OA and its effects in the future.

LITERATURE CITED

Calhoun, S. K.; Haas, A. F.; Takeshita, Y.; Johnson, M.; Fox, M.; Smith, J.; Mueller, B.; Vermeij, M.; Rohwer, F. L.; Nightime Dissolved Oxygen Spikes Across Coral Reef Environments: Biological or Not?

Cesar, Herman SJ, Pieter Van Beukering, Sam Pintz, and Jan Dierking. 2004. Economic valuation of the coral reefs of Hawai'i. Pacific Science: Volume 58, No. 2, pg. 231-242.

De Putron, S. J., McCorkle, D. C., Cohen, A. L., & Dillon, A. B. 2011. The impact of seawater saturation state and bicarbonate ion concentration on calcification by new recruits of two Atlantic corals. Coral Reefs, Volume 30, No. 2, pg. 321-328.

Drupp, Patrick S., Eric Heinen De Carlo, Fred T. Mackenzie, Christopher L. Sabine, Richard A. Feely, and Kathryn E. Shamberger. 2013. Comparison of CO2 Dynamics and Air–Sea Gas Exchange in Differing Tropical Reef Environments. Aquatic Geochemistry: Volume 19, No. 5-6. pg 371-397.

Fabry, Victoria J., Brad A. Seibel, Richard A. Feely, and James C. Orr. 2008. Impacts of ocean acidification on marine fauna and ecosystem processes. ICES Journal of Marine Science: Journal du Conseil: Volume 65, No. 3. pg. 414-432.

Feely, Richard A., Christopher L. Sabine, Kitack Lee, Will Berelson, Joanie Kleypas, Victoria J. Fabry, and Frank J. Millero. Impact of anthropogenic CO2 on the CaCO3 system in the oceans. Science: Volume 305, No. 5682. pg. 362-366.

Feely, Richard A., Scott C. Doney, and Sarah R. Cooley. 2009. Ocean acidification: present conditions and future changes in a high-CO2 world.

Hendriks, Iris E. 2014. Photosynthetic activity buffers ocean acidification in seagrass meadows. Biogeosciences. Volume 11, No. 2, pg. 333-346.

Kroeker, Kristy J., et al. 2010. Meta- analysis reveals negative yet variable effects of ocean acidification on marine organisms. Ecology letters. Volume 13, No. 11 pg. 1419-1434.

Orr, JC, VJ Fabry, O Aumont et al. 2005. Anthropogenic ocean acidification over the twenty first century and its impacts on calcifying organisms. Nature: Volume 437, pg 681-686.

Pelletier, G. J., E. Lewis, and D. Wallace. 2007. CO2SYS. XLS: A calculator for the CO2 system in seawater for Microsoft Excel/VBA, Wash. State Dept. of Ecology/Brookhaven Nat. Lab., Olympia, WA/Upton, NY, USA.

Roleda, Michael Y., Philip W. Boyd, and Catriona L. Hurd. 2012. Before ocean acidification: calcifier chemistry lessons1. Journal of Phycology. Volume 48, No. 4, pg. 840-843.

Willette, T. Mark, et al. 2001. Ecological processes influencing mortality of juvenile pink salmon (Oncorhynchus gorbuscha) in Prince William Sound, Alaska. Fisheries Oceanography. Volume 10, No. 1, pg. 14-41.

Wootton, J. Timothy, Catherine A. Pfister, and James D. Forester. 2008. Dynamic patterns and ecological impacts of declining ocean pH in a high-resolution multi-year dataset. Proceedings of the National Academy of Sciences: Volume 105, No. 48. pg 18848-18853.

Yasunaka, Sayaka, et al. 2014. Mapping of sea surface nutrients in the North Pacific: Basin- wide distribution and seasonal to interannual variability. Journal of Geophysical Research: Oceans. Volume 119, No. 11, pg. 7756-7771.